RAA 2014 Vol. **14** No. **1**, 35–46 doi: 10.1088/1674–4527/14/1/003
http://www.raa-journal.org *http://www.iop.org/journals/raa*

Research in Astronomy and Astrophysics

Time-resolved spectral analysis of prompt emission from long gamma-ray bursts with GeV emission

Arikkala Raghurama Rao[1], Rupal Basak[1], Jishnu Bhattacharya[2], Sarthak Chandra[2], Nikunj Maheshwari[3], Manojendu Choudhury[4] and Ranjeev Misra[5]

[1] Tata Institute of Fundamental Research, Mumbai 400005, India; *arrao@tifr.res.in*
[2] Indian Institute of Technology, Kanpur 208016, India; *jishnuonline@gmail.com*
[3] Indian Institute of Technology, Mumbai 400076, India; *nikunj029@gmail.com*
[4] Centre for Excellence in Basic Sciences, Mumbai 400098, India; *nikunj029@gmail.com*
[5] Inter-University Centre for Astronomy and Astrophysics, Pune 411007, India; *rmisra@iucaa.ernet.in*

Received 2013 May 27; accepted 2013 August 9

Abstract We performed detailed time-resolved spectroscopy of bright long gamma-ray bursts (GRBs) which show significant GeV emissions (GRB 080916C, GRB 090902B and GRB 090926A). In addition to the standard Band model, we also use a model consisting of a black body and a power law to fit the spectra. We find that for the latter model there are indications of an additional soft component in the spectra. While previous studies have shown that such models are required for GRB 090902B, here we find that a composite spectral model consisting of two blackbodies and a power law adequately fits the data of all the three bright GRBs. We investigate the evolution of the spectral parameters and find several interesting features that appear in all three GRBs, like (a) temperatures of the blackbodies are strongly correlated with each other, (b) fluxes in the black body components are strongly correlated with each other, (c) the temperatures of the black body trace the profile of the individual pulses of the GRBs, and (d) the characteristics of power law components like the spectral index and the delayed onset bear a close similarity to the emission characteristics in the GeV regions. We discuss the implications of these results and the possibility of identifying the radiation mechanisms during the prompt emission of GRBs.

Key words: gamma rays: bursts – gamma rays: observations – methods: data analysis

1 INTRODUCTION

Gamma-ray bursts (GRBs) are some of the most energetic events that are detected in astronomical observations, with emissions spanning several decades of energy, from a few tens of keV to tens of GeVs (see, e.g. Abdo et al. 2009a). The origin of the bursting mechanism as well as the radiative processes that give rise to the emission is still a matter of intense debate (Zhang 2007; Dado & Dar 2009). Although there is a great variety in the shapes of the light curves observed, the bursts have historically been classified into short and long as per the duration of the prompt emission. The former has a duration of less than 2 s while long GRBs can last from a few seconds to hundreds of seconds.

Recently there have been efforts to account for the diverse spectral and temporal properties as well as the location and classify them into Type I and Type II cases (Zhang 2007; Zhang et al. 2009). Both types show afterglows in lower energy bands (ranging from X-rays to radio) that may last from days to weeks (see Gehrels et al. 2009 for a general review of GRBs).

The approach for investigating the working mechanism of a GRB involves two independent paradigms: first, the theoretical assumption and/or the simulation of a central engine along with the processes that may lead to the outburst and/or the subsequent emission processes followed by phenomenological fitting of the data by the assumed models (Goodman 1986; Paczynski 1986; Dar 2006; Dado et al. 2007; King 2007; Pugliese et al. 1999; Metzger et al. 2011; Zhang & Mészáros 2002), and second, the data driven analysis of observed processes (Band et al. 1993; Amati et al. 2002; Ackermann et al. 2010). Presupposition of a theoretical scenario may at times induce a bias in the analysis process and the subsequent interpretation of the data, while the data driven reasoning may at times lead to either empirical or unphysical explanations.

Long GRBs provide an opportunity to analyze the time-resolved spectra of the prompt emission with a comparative statistical advantage over short GRBs. The challenge of such an analysis lies in fitting the data with a physically meaningful model, in contrast to the Band model (Band et al. 1993) which provides a very good statistical fit to the data with two power law components smoothly joined at the peak energy. In an attempt to fit more physically meaningful models, Ryde (2004, 2005) and Ryde & Pe'er (2009) have fitted the time-resolved spectra of clear, fast rise exponential decay pulses of BATSE GRBs with a black body and a power law. The data quality produced by the detectors was not suitable for more nuanced analysis. Recently many attempts have been made to mimic the Band model by more physically relevant models (Ackermann et al. 2011), and there have also been efforts to extend the Band model into the very high energy gamma-ray as well as the less then 50 keV X-ray regime of the electromagnetic spectrum (Abdo et al. 2009b).

The observational analysis of GRBs received a boost with the launch of the Fermi satellite observatory. The Fermi Gamma-ray Space Telescope hosts two instruments, the Large Area Telescope (LAT, 20 MeV to more than 300 GeV, Atwood et al. 2009) and the Gamma-ray Burst Monitor (GBM, 8 keV–40 MeV, Meegan et al. 2009), which together are capable of measuring the spectral parameters of GRBs across seven decades in energy. One of the remarkable observations from the Fermi satellite is the detection of high energy ($\sim$GeV) emission from GRBs. Detection of photons up to an energy of 30 GeV constrained the Lorentz factor of the jet to be greater than ~ 1000 (Abdo et al. 2009a; Ghirlanda et al. 2010a); detection of GeV photons from the short GRB 090510 helped put stringent limits on the violation of Lorentz invariance (Abdo et al. 2009c). Although the detection of a large number of photons above 100 MeV ($>$100) in some of the bright GRBs like GRB 090902B helped compile detailed time resolved spectroscopy, no unified spectral model explaining the prompt emission of GRBs across the full energy range has yet emerged. For example, GRB 090902B shows a separate peaked Band emission in the 50 keV – 1 MeV region and a power law connects the > 100 MeV emission (Abdo et al. 2009b) whereas GRB 080916C shows a single Band function fitting across the full energy range (Abdo et al. 2009a). A detailed time-resolved study of 17 GRBs with high energy emission showed the possibility of five spectral combinations to explain the data (Zhang et al. 2011).

Ryde et al. (2010) have found that the time-resolved spectra of GRB 090902B do not agree with the physically meaningful model of a black body and a power law, but a continuous distribution of temperature fits the data. The need for such more complex models to fit the data may lead the way to a better understanding of the radiative processes responsible for the prompt emission and to distinguish different dynamical models. However, it may also be possible that such complexities only exist for certain GRBs and hence inferences drawn from such studies may not be general. Indeed, Ryde et al. (2010) suggest that in other GRBs, like GRB 080916C, the thermal component may be lacking. It is important to know whether a single empirical model can fit the time-resolved spectra of all GRBs that have sufficiently good signal to noise data.

In this paper, we report the results of time-resolved spectral analyses of three long GRBs which have shown intense GeV emissions and which are also bright in the 1 keV–10 MeV range (fluence $> 10^{-4}$ erg cm^{-2}). Our aim is to find a spectral model which can be used to describe the time-resolved spectral data and connect the spectral parameters to the high energy emission. Our approach is data driven, our interpretation is phenomenological and our attempt is to look for an empirical model that fits the time-resolved spectra of all bright GRBs. In Section 2, we describe the data we used for our analysis, and the softwares we used. In Section 3, we describe the details of the time-resolved spectral analysis of the light curves of the three GRBs. In Section 4, we present our results followed by a discussion.

2 DATA SELECTION AND EXTRACTION

Zhang et al. (2011) have made a systematic time-resolved spectral analysis of a complete sample of 17 GRBs with Fermi LAT detection (another six are added to this list based on a systematic search of the Fermi-LAT database using a matched filter technique – see Zheng et al. 2012). The complete details of all these GRBs are also given in the Fermi-LAT Collaboration (2013). We have selected three long GRBs from this list which are bright in MeV (fluence $> 10^{-4}$ erg cm^{-2}) and GeV regions ($>$100 photons above 100 MeV). Only one other GRB in this list has intense GeV emission, but it is a short GRB with comparatively lower fluence (GRB 090510 with a fluence of 2 $\times 10^{-5}$ erg cm^{-2} and duration of 0.3 s). These three GRBs show a delayed onset of > 100 MeV emission (see also Ackermann et al. 2011; Abdo et al. 2009a,b,c).

The Fermi satellite has two detectors, namely the GBM and the LAT. The GBM is the primary instrument for the detection and study of GRB prompt emission. It detects X-rays and low energy γ-rays. It has two scintillation detectors: the sodium iodide (NaI) detector is sensitive in the range ~ 8 keV to ~ 900 keV while the BGO detector is in the range ~ 200 keV to ~ 40 MeV (Meegan et al. 2009). The other primary detector onboard Fermi is the LAT. It has a large field of view, such that it can see 20% of the entire sky at any time, and over a period of 3 hours it scans the whole sky. The effective area of LAT is 9500 cm^2. For both detectors, we used data which were publicly available at the Fermi mission website[1].

We used the standard procedure for the GBM analysis, closely following the method described in Basak & Rao (2012a,b). For each GRB we used two or more NaI detectors with high detected count rates, according to the data present in the "Time Tagged Event" (TTE) file. We chose one BGO detector depending on the selected NaI detectors. If NaI detectors 1–6 were selected we used BGO 0, else we used BGO 1. For ambiguous cases, we used the BGO which showed a higher count rate. We used the TTE file to extract the light curves and spectra. Using the spectral analysis tool RMFIT (version 3.3pr7), developed by user contributions to the Fermi Science Support Center, we created the time bins from the original TTE file to reduce the fluctuations. After binning, we fitted a linear or a cubic polynomial to the background, by choosing time intervals before and after the prompt emission phase. For the time resolved spectral analysis, we followed the method of Basak & Rao (2013) and selected time bins with fixed excess counts: we repeated the analysis with total excess counts of ~ 2000 and ~ 4000 for GRB 090902B. Since we derived consistent results with these count rates, we used an excess count of ~ 2000 for the analysis of the other two GRBs. We grouped the spectral files, the response files and the background files such that in each spectral bin a sufficient number of counts are available for good statistics (typically 40 counts for NaI detectors and 50–60 counts for the BGO detectors) and analyzed the data with the spectral analysis software XSPEC (Version 12.7.0).

For analyzing the LAT data, we used the LAT ScienceTools–v9r23p1 package. We also used the "transient" response function. We have considered the time periods for which the signal to noise ratio is relatively high, and the data lost due to inadequate signal is not significant. We chose the LAT

[1] *http://fermi.gsfc.nasa.gov/ssc/data/access*

Table 1 GRB Coordinates, Trigger Time and the GBM Detector Numbers

GRB	RA (J2000) (h m s)	Dec (J2000) (° ′ ″)	Trigger Time (UT)	NaI	BGO
080916C	07 59 23	− 56 38 20.1	00:12:45.61	3, 4	0
090902B	17 38 00	+27 19 26.6	11:05:08.31	0, 9	1
090926A	23 33 36	−66 19 25.9	04:20:41.00	3, 7	1

data based on the time and position measured by other detectors like the GBM. We downloaded the data from the Fermi-LAT database (the "LAT Weekly Files") from the NASA HEASARC website, using the precise GRB coordinates available in the literature. To filter out the emission coming from the Earth's atmosphere due to cosmic rays, we used a maximum zenith angle cutoff value of 105°. We binned the data in time using the tool gtbin provided by the NASA ScienceTools package. We chose the energy range from 100 MeV–300 GeV, and obtained the light curves. For the spectral analysis, we found that the uncertainties in the data beyond 2 GeV were large. We considered the energy range from 30 MeV–2 GeV for spectral fitting.

For the three GRBs studied here, the coordinates, trigger time and GBM detectors used for the analysis are listed in Table 1.

3 TIME-RESOLVED SPECTRAL ANALYSIS

GRB 090902B is the brightest of the three selected GRBs and we first attempt a time-resolved spectral analysis of this GRB. The light curve of the prompt emission has multiple peaks in all the energy bands (see for example Abdo et al. 2009b; Fermi-LAT Collaboration 2013) with two prominent peaks. The LAT counts are delayed by about 3 s compared to the counts in the GBM. The time-resolved spectra have been fitted by Abdo et al. (2009b) where they extended the Band model with a power law that continues to below 50 keV and above to gamma-rays with very high energy (in the GeV regime). Zhang et al. (2011) found that the Band model becomes increasingly narrower with smaller time intervals and they concluded that a black body and a power law give a correct description of the time-resolved spectra, though other models like power law with a cutoff could also fit the data. They, however, concluded that the blackbody and a power law are unique to this source and there is no evidence for such a combination in other GRBs. Ryde et al. (2010) could derive acceptable fits to the time resolved spectra using a composite model involving a multi-color blackbody and a power law. The blackbody temperature is a continuous distribution with the flux at each temperature having a power-law relation with temperature up to a maximum temperature, $T_{\rm max}$.

In our attempt to arrive at an acceptable time resolved spectral model for the bright GRBs, we first fit the time resolved GBM data (with ~ 2000 counts per spectrum) with the "blackbody + power law" model (hereafter referred to as the BBPL model). We found high values for the reduced χ^2 (χ^2_r), particularly during the rising part of the pulse features.

In Figure 1 we show a representative example of one of the spectra. When we only fit with a Band model, we get a high χ^2, which improves for the BBPL model, but there are still residuals, particularly at the peak of the spectrum. When we include another blackbody (the lower blackbody has a temperature $kT \sim$ a few tens of keV, while the higher blackbody has $kT > 100$ keV) along with a power law (hereafter referred to as the 2BBPL model), we find a very significant improvement in the value of χ^2_r. The improvement to the fit is shown graphically in Figure 2 for the time resolved spectral analysis. The average value of χ^2_r is 1.47 for the Band model fitting (with a dispersion of 0.65) and it improves to 1.41 for a blackbody with a power law. The addition of another blackbody component improves the χ^2_r to 1.05 (average value) with a dispersion of 0.15. The power-law index Γ has an average value of 1.76 with a dispersion of 0.17 (shown in the bottom panel of Fig. 3). When we use a continuous distribution of temperature (hereafter called the mBBPL model) with the time

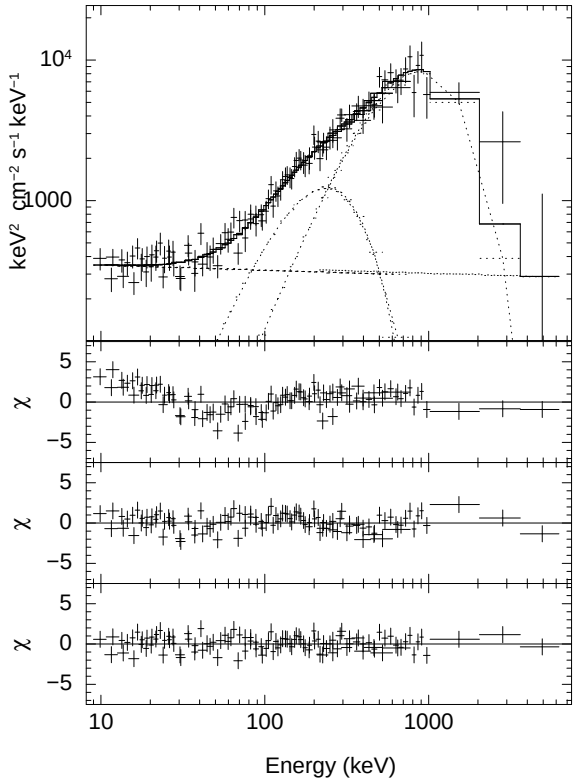

Fig. 1 Unfolded energy spectrum of a time-resolved spectrum of GRB 090902B using a model consisting of two blackbodies and a power law (2BBPL model) shown in the top panel. Individual model components are shown as dotted lines. The residuals to the fit are shown in the bottom three panels for (successively from the top) the Band model, blackbody and a power-law (BBPL model) and the 2BBPL model.

resolved data (as was done by Ryde et al. 2010), we find that data are consistent with this model (χ^2_r = 1.14 with a dispersion of 0.15). We find that the LAT spectra are fitted satisfactorily by a power-law model with the power-law index obtained from the GBM time-resolved analysis. Zhang et al. (2011) report a LAT power-law index of 1.76 for this GRB.

The evolution of spectral parameters for GRB 090902B is shown in Figure 3, left panels. The temperatures of the two blackbodies are plotted in the top panel and the flux values in the individual components are shown in the next panel. The most interesting observation here is the evolution of the two temperatures, which exactly follows the same trend, suggesting that a single phenomenon is driving their evolution. In Figure 4, left panel, a scatterplot of the individual temperatures of the two blackbodies is shown. A good level of correlation (correlation coefficient, r, of 0.96 for 48 data points) is seen and a slope of 0.29$\pm$0.04 is obtained. The normalizations of the two blackbodies are also correlated with each other.

Following Ryde & Pe'er (2009) we have defined a dimensional photospheric radius parameter $R_{\rm p}$ as

$$R_{\rm p} = \left(\frac{F_{\rm BB}}{\sigma T^4}\right)^{1/2}, \quad (1)$$

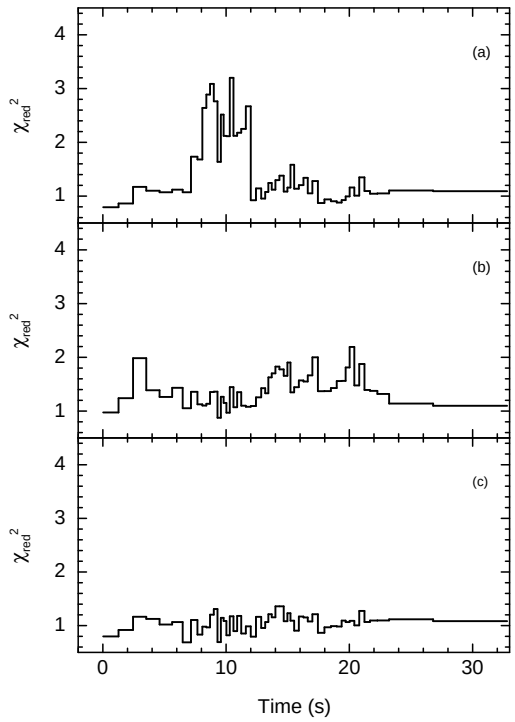

Fig. 2 The average values of reduced χ^2 are 1.47, 1.41 and 1.05, respectively for panels (a), (b) and (c) and the rms deviations in them are 0.65, 0.29 and 0.15, respectively for the three panels.

where $F_{\rm BB}$ is the blackbody flux, T is the temperature of the blackbody and σ is the Stefan-Boltzmann constant. $R_{\rm p}$ is proportional to the photospheric emission radius for a GRB of given redshift and Lorentz factor (see eqs. (3) and (4) in Ryde & Pe'er 2009). $R_{\rm p}$ is plotted in Figure 3, for both of the blackbodies in the 2BBPL model. Since the temperatures and fluxes are correlated and show similar slopes (about 0.3), $R_{\rm p}$ for the low temperature blackbody is a factor of six higher than that of the high temperature blackbody. Although the GRBs considered here do not have clear pulse structures, an increasing trend of $R_{\rm p}$ can be seen in the figure.

The light curve of the prompt emission from GRB 090926A has multiple peaks in all the energy bands (see for example Ackermann et al. 2011). The LAT counts are delayed by about 5 s compared to the counts in the GBM. The time resolved spectra have been fitted by Ackermann et al. (2011) where they have extended the Band model with a cutoff-power law, reporting a spectral break at around 1.4 GeV, while claiming that this additional component is more prominent than the Band component. In our attempt to fit the time-resolved spectra (taken with total source counts of $\sim$ 2000 in each time bin) with the BBPL model, again we were unable to find a proper fit, whereas two blackbodies (the lower blackbody has a temperature $kT \sim$ few tens of keV, while the higher blackbody has a $kT > 100$ keV) along with a power law did also provide adequate and acceptable fit statistics for this source.

In Figure 3 (right panels) the temperature and flux evolutions for GRB 090926A are shown. The LAT spectra are fitted satisfactorily by a power-law model with the power-law index obtained from the GBM data, though Zhang et al. (2011) report a power-law index of 2.03 for this source in the LAT energy range. Again, the change in the power-law flux appears to drive the LAT light curve.

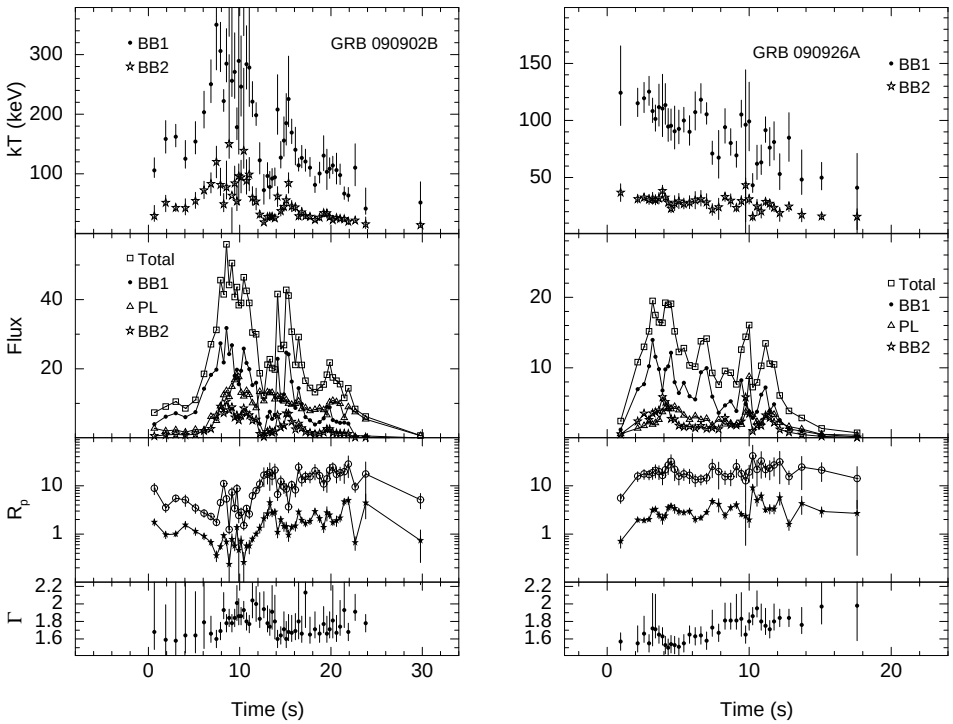

Fig. 3 The variation of the parameters for a time resolved spectral analysis of GRB 090902B using the 2BBPL model is shown in the left panels of the figure. The panels, successively from top, show the temperatures of the two blackbody components; fluxes (in units of 10^{-6} erg cm^{-2} s^{-1}) in various components; the dimensionless photospheric radius parameter $R_{\rm p}$ (see text) in units of 10^{-19} for the higher blackbody (*stars*) and lower blackbody (*open circles*); and the power-law index. Similar quantities for GRB 090926A are shown in the right panels of the figure.

Also for this source, the most interesting observation is the evolution of the two temperatures, which follows exactly the same trend, suggesting that a single phenomenon is driving their evolution. A scatterplot of the two temperatures is shown in Figure 4, right panel. A good level of correlation (correlation coefficient, r, of 0.81 for 36 data points) is seen and a slope of 0.22$\pm$0.06 is obtained. The normalizations of the blackbody components are also correlated with each other.

For GRB 080916C, the LAT light curve reached its peak a few seconds after the trigger, whereas the GBM light curve reached its peak immediately after the trigger (Abdo et al. 2009a). The delay between the GBM and LAT counts for this source is about 4 s. For the time resolved spectral study we find that the Band model provides a better fit compared to the BBPL model. In our attempt to identify a uniform spectral distribution for diverse GRBs, we followed the method of Basak & Rao (2013) and did a uniform analysis for all the three GRBs. We selected three episodes in GRB 090902B (0–7.2 s, 7.2–12 s and 12–35.2 s, respectively – see Fig. 2) and the other two GRBs. We made a simultaneous fit to the time resolved spectral files with the following constraints: (a) indices α and β are tied for the Band model; (b) power-law indices are tied in the BBPL model; (c) power-law index and the temperature variation index are tied in the mBBPL model; and (d) power-law index and the ratio of temperatures and normalizations are tied in the 2BBPL model. The resultant reduced χ^2 values are shown in Table 2. We can conclude that the 2BBPL model gives a uniformly good fit to the data for all three GRBs.

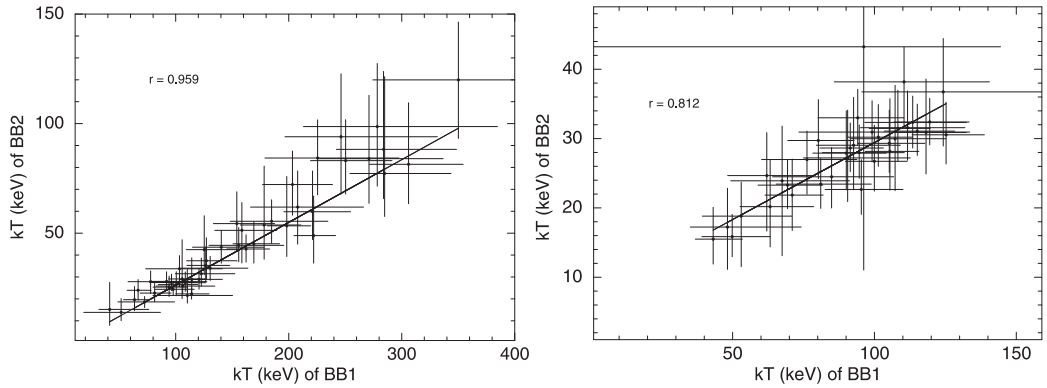

Fig. 4 The scatterplot of the temperature (kT) of the higher blackbody component with the temperature (kT) of the lower blackbody for GRB 090902B (*left panel*) and GRB 090926A (*right panel*). The correlation coefficients, r, are indicated in the panels. The straight lines show linear fits to the data.

Table 2 The Reduced χ^2 Values for the Various Models

GRB	Band	BBPL	mBBPL	2BBPL
080916C	1.05	1.14	1.07	1.04
090902B (0–7.2 s)	1.19	1.38	1.10	1.11
090902B (7.2–12 s)	3.81	1.25	1.15	1.16
090902B (12–35.2 s)	1.33	1.65	1.24	1.22
090926A	1.11	1.68	1.19	1.15

3.1 Evolution of the Power-law Flux

An examination of the flux evolution for all the three GRBs shows that the power-law flux has a delayed start and the blackbody temperature and flux decrease sharply towards the end of the burst. To investigate the evolution of the flux beyond the prompt emission, we have obtained the spectral data with long integration times in four bins for GRB 090902B (25–30 s, 30–40 s, 40–60 s and 60–100 s, respectively), three bins for GRB 090926A (17–30 s, 30–50 s and 50–70 s, respectively) and one bin for GRB 080916C (64–100 s). We fit a power law to the GBM data with the value of the index frozen at the average values obtained from the time resolved analysis of the prompt emission. We investigate below whether the power-law flux in the GBM range (reflecting the non-thermal part of the prompt emission) is related to the LAT flux (which is assumed to have a non-thermal origin).

In Figure 5 we show the evolution of the power-law flux (shown as open boxes, in the units of 10^{-6} erg cm^{-2} s^{-1}) along with the LAT flux (shown as stars, in the units of LAT count rates $>$100 MeV). It is quite fortuitous that the choice of these units makes the quantities have a similar range of values. The LAT boresight angles for these three GRBs are quite similar to each other (49°, 50° and 47°, respectively for GRB 080916C, GRB 090902B and GRB 090926A – see Zheng et al. 2012) and hence the observed count rates can be regarded as the relative LAT fluxes for a given GRB. It can be seen that the power-law flux tracks the LAT flux quite well. For GRB 090902B, the power-law flux is a factor of 10 lower than the peak flux in the initial 6 s after the trigger and the rise thereafter coincides quite smoothly with the rise in the LAT flux. The first peaks (at 9–11 s) in the two energy ranges also coincide with each other, though the fall after 20 s is much steeper for the power-law flux. In GRB 090926A, on the other hand, the power-law flux, though delayed ($\sim$ 3 s)

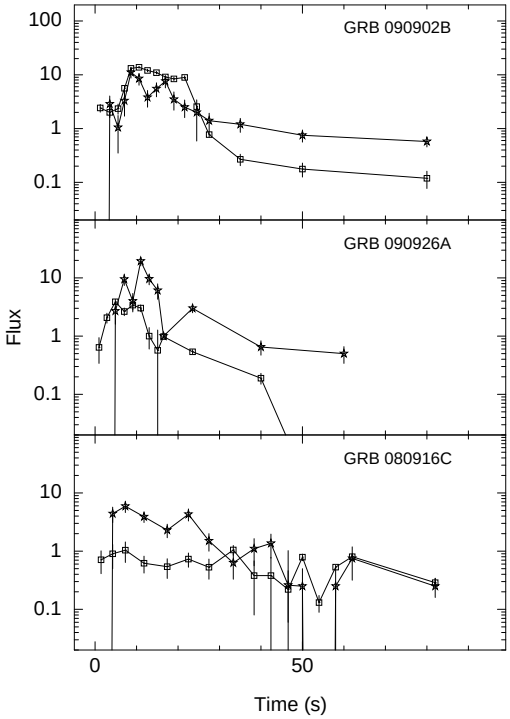

Fig. 5 The variation of the power-law flux (in units of 10^{-6} erg cm^{-2} s^{-1}) for the time resolved spectral analysis using the 2BBPL model (*open squares*) and the LAT flux (shown as *stars*, in units of the observed LAT count rates for events above 100 MeV) shown as a function of time for GRB 090902B (*top panel*), GRB 090926A (*middle panel*) and GRB 080916C (*bottom panel*).

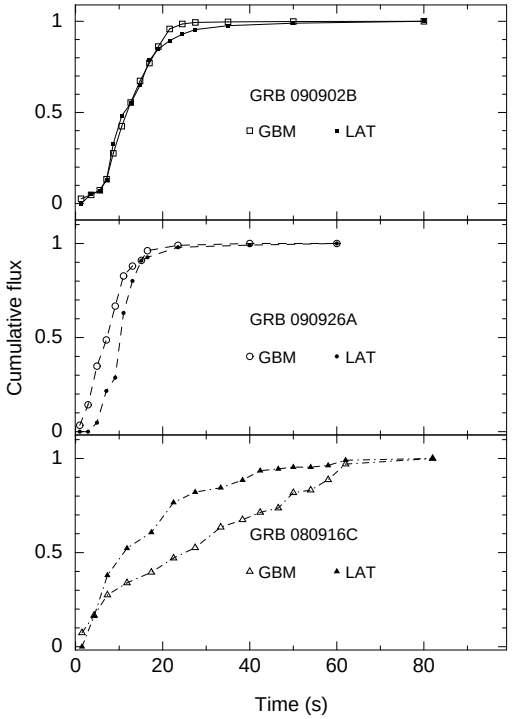

Fig. 6 The cumulative integrated flux distribution for GBM power-law flux (*open symbols*) shown along with a similar distribution for the LAT flux (*filled symbols*) for GRB 090902B (*top panel*), GRB 090926A (*middle panel*) and GRB 080916C (*bottom panel*).

rises earlier than the LAT flux (~ 5 s). In GRB 080916C the two fluxes track each other remarkably well, including a dip in both the fluxes at ~ 55 s after the trigger. Cumulative flux distributions which highlight the similarities in the trends during the rising phase of each GRB are shown in Figure 6.

In Figure 7 we show a scatterplot of the LAT flux against GBM power-law flux for all the three GRBs. The two fluxes are correlated very well for GRB 090902B (correlation coefficient, r, of 0.84 for 16 data points) and weakly correlated for the other two GRBs (r of 0.32 and 0.36, respectively for GRB 090926A and GRB 080916C).

4 DISCUSSION AND CONCLUSIONS

The time-integrated as well as the time-resolved spectra of GRBs are traditionally fitted with the Band model, in which two power laws smoothly join together (see e.g. Nava et al. 2011; Ghirlanda et al. 2010b). The existence of power laws immediately points towards some non-thermal phenomena, but the variations in the Band spectral parameters with time, for a given GRB, are quite difficult to reconcile with any reasonable physical scenario of non-thermal radiation mechanisms (see for example Ghirlanda et al. 2003). There have been attempts to model the time-resolved spectra of GRBs with some sort of photospheric thermal emissions (Ryde 2004, 2005), but the variations of the pa-

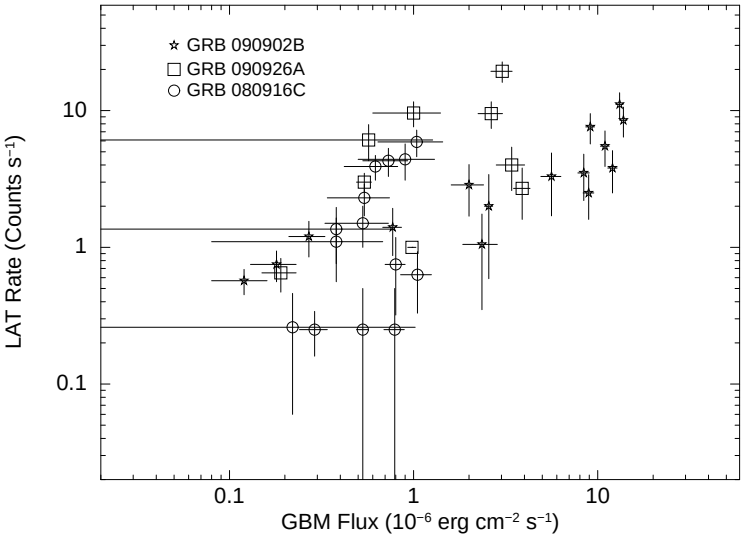

Fig. 7 A scatterplot of the power-law flux in the 2BBPL model with the LAT count rates for a time resolved analysis of GRB 090902B (*stars*), GRB 090926A (*squares*) and GRB 080916C (*circles*).

rameters like the blackbody temperature with time show some increase in the initial parts which are quite difficult to reconcile with any physical scenario.

In the present work we have demonstrated that a model consisting of two blackbodies and a power law adequately fits the time-resolved data. We have further shown that this model gives a statistically better fit compared to other models, when all the three GRBs are considered. Considering the fact that this model is also the preferred one for bright GRBs with single/separable pulses (Basak & Rao 2013), we can conclude that such a composite model also needs to be examined for other GRBs. This spectral description has several attractive features which can be used to constrain the GRB emission mechanism. The advantages of using the 2BBPL model are listed below.

(1) GRB 090902B is not unique: All the three bright LAT detected GRBs are also consistent with the 2BBPL model.
(2) Physically reasonable non-thermal component: The data are consistent with a power law with the same index for a given GRB. Hence, phenomenological explanations in terms of non-thermal phenomena like shock acceleration are easy to implement.
(3) Well behaved variation in the thermal component, including the initial parts of the GRB pulses.
(4) Non-thermal component closely matches the LAT emission.

If the 2BBPL model is the correct description of a GRB, it has the following implications.

First, the existence of two closely correlated blackbody temperatures (with a similar ratio of temperature for different GRBs) provides a unique handle to pin down the radiation mechanism. If they are due to two distinct locations in the photosphere, variation of temperature gives the cooling mechanism. If these two temperatures are due to two coexisting glories of photons as per the cannonball model (Dado et al. 2007), one can identify the higher temperature with the typical photon field in the pre-supernova region (a few eV boosted to ~ 100 keV by the cannonball with a large bulk Lorentz factor, Γ_0) and the lower temperature could be the photon field generated by some other process like bremsstrahlung. A correct identification of these two temperatures will provide a good handle on Γ_0 and measuring such parameters for the different pulses of a given GRB can provide other useful jet

parameters like the beaming angle. In the fireball scenario, on the other hand, thermal emission in the photosphere will have an angular dependence and a range of temperatures is expected, and hence the multicolor blackbody description (the mBBPL model) would be a better alternative. As can be seen from Table 2, the mBBPL and 2BBL models give almost equally satisfactory results.

Second, the non-thermal component can be described as a power law with a constant or slowly varying index, extending all the way to GeV energies (though we cannot completely rule out spectral breaks/change in index from the MeV to the GeV region). The bulk of the initial prompt energy is in the thermal components and a smoothly varying non-thermal component across the MeV to GeV range should be quite easy to handle (see for example Barniol Duran & Kumar 2011). In the case of GRB 090902B, the average spectral index of the power law in the MeV region (1.76 ± 0.17) for the 2BBPL model agrees very well with the index obtained in the GeV region (1.76), whereas for GRB 090926A the average index (1.65 ± 0.35) differs from that derived in the GeV region (2.03). Hence we cannot completely rule out a spectral break from the MeV to the GeV region.

We would like to point out that there are several observational features in the GRB prompt emission which indicate the possibility of a separate thermal component rather than a continuous temperature distribution. Guiriec et al. (2011) found that GRB 100724B requires an additional thermal component at ~ 38 keV. Considering the fact that the $E_{\rm peak}$ for this GRB was reported to be 350 keV (which is equivalent to a thermal spectrum of $kT \sim 117$ keV, since the thermal spectrum peaks at 3 kT), the derived ratio of temperatures (~ 3) is quite similar to what we found in the present work. Shirasaki et al. (2008) identified a low energy component which can be modeled as a blackbody in GRB 041006 and the variations of the peak energy in the multiple components in the time-resolved spectra are found to be related to each other. Preece et al. (1996) analyzed the low energy data from the BATSE spectroscopic detectors and identified a low energy component in 15% of the bursts. It is quite conceivable that the existence of two blackbodies with correlated behavior is a feature in all GRBs and they become evident in the data of bright GRBs with very high peak energy (so that both blackbodies are within the $\sim 10 - 1000$ keV region).

Finally, the utility of the classical Band spectrum can be understood as a collection of evolving BBPL/2BBPL spectra, and a smoothly evolving thermal spectrum is a good approximation to the Band model. The fact that for sources like GRB 090926A, the Band model gives a good fit to the time resolved data, comparable to the 2BBPL model, could be an indication that the Band model effectively captures an evolving blackbody spectrum (evolving within the time bin) better than the 2BBPL model with a constant temperature (within the bin). An empirical description of an evolving 2BBPL model and developing a spectral model with such empirical description and testing them with the data could be a way to understand the time-resolved spectra of GRBs.

Acknowledgements This research has made use of data obtained through the HEASARC Online Service, provided by NASA/GSFC, in support of NASA High Energy Astrophysics Programs. We thank the anonymous referee for very useful comments.

References

Abdo, A. A., Ackermann, M., Arimoto, M., et al. 2009a, Science, 323, 1688
Abdo, A. A., Ackermann, M., Ajello, M., et al. 2009b, ApJ, 706, L138
Abdo, A. A., Ackermann, M., Ajello, M., et al. 2009c, Nature, 462, 331
Ackermann, M., Ajello, M., Baldini, L., et al. 2010, ApJ, 717, L127
Ackermann, M., Ajello, M., Asano, K., et al. 2011, ApJ, 729, 114
Amati, L., Frontera, F., Tavani, M., et al. 2002, A&A, 390, 81
Atwood, W. B., Abdo, A. A., Ackermann, M., et al. 2009, ApJ, 697, 1071
Band, D., Matteson, J., Ford, L., et al. 1993, ApJ, 413, 281
Barniol Duran, R., & Kumar, P. 2011, MNRAS, 417, 1584

Basak, R., & Rao, A. R. 2012a, ApJ, 745, 76
Basak, R., & Rao, A. R. 2012b, ApJ, 749, 132
Basak, R., & Rao, A. R. 2013, ApJ, 768, 187
Dado, S., & Dar, A. 2009, in American Institute of Physics Conference Series, eds. G. Giobbi, A. Tornambe, G. Raimondo, M. Limongi, L. A. Antonelli, N. Menci, & E. Brocato, 1111, 333
Dado, S., Dar, A., & De Rújula, A. 2007, ApJ, 663, 400
Dar, A. 2006, Chinese Journal of Astronomy and Astrophysics Supplement, 6, 301
Fermi-LAT Collaboration 2013, arXiv:1303.2908
Gehrels, N., Ramirez-Ruiz, E., & Fox, D. B. 2009, ARA&A, 47, 567
Ghirlanda, G., Celotti, A., & Ghisellini, G. 2003, A&A, 406, 879
Ghirlanda, G., Nava, L., & Ghisellini, G. 2010a, A&A, 511, A43
Ghirlanda, G., Ghisellini, G., & Nava, L. 2010b, A&A, 510, L7
Goodman, J. 1986, ApJ, 308, L47
Guiriec, S., Connaughton, V., Briggs, M. S., et al. 2011, ApJ, 727, L33
King, A. 2007, Royal Society of London Philosophical Transactions Series A, 365, 1277
Meegan, C., Lichti, G., Bhat, P. N., et al. 2009, ApJ, 702, 791
Metzger, B. D., Giannios, D., Thompson, T. A., Bucciantini, N., & Quataert, E. 2011, MNRAS, 413, 2031
Nava, L., Ghirlanda, G., Ghisellini, G., & Celotti, A. 2011, A&A, 530, A21
Paczynski, B. 1986, ApJ, 308, L43
Preece, R. D., Briggs, M. S., Pendleton, G. N., et al. 1996, ApJ, 473, 310
Pugliese, G., Falcke, H., & Biermann, P. L. 1999, A&A, 344, L37
Ryde, F. 2004, ApJ, 614, 827
Ryde, F. 2005, ApJ, 625, L95
Ryde, F., & Pe'er, A. 2009, ApJ, 702, 1211
Ryde, F., Axelsson, M., Zhang, B. B., et al. 2010, ApJ, 709, L172
Shirasaki, Y., Yoshida, A., Kawai, N., et al. 2008, PASJ, 60, 919
Zhang, B. 2007, ChJAA (Chin. J. Astron. Astrophys.), 7, 1
Zhang, B., & Mészáros, P. 2002, ApJ, 581, 1236
Zhang, B., Zhang, B.-B., Virgili, F. J., et al. 2009, ApJ, 703, 1696
Zhang, B.-B., Zhang, B., Liang, E.-W., et al. 2011, ApJ, 730, 141
Zheng, W., Akerlof, C. W., Pandey, S. B., et al. 2012, ApJ, 756, 64